Angle-resolved photoelectron spectroscopy study of the surface electronic structure of ZnTe(110)

H. Qu, J. Kanski, and P. O. Nilsson
Department of Physics, Chalmers University of Technology, S-412 96 Göteborg, Sweden

U. O. Karlsson
MAX-lab, Lund University, Box 118, S-221 00 Lund, Sweden
(Received 17 August 1990; revised manuscript received 6 December 1990)

The valence-electronic structure of the ZnTe(110) surface has been studied by angle-resolved photoelectron spectroscopy using synchrotron radiation. The bulk valence bands and, in particular, the energies at the Γ and X points have been extracted from normal-emission data. Several surface-related structures have been identified in off-normal-emission data, from which band structures of surface states and resonances have been derived.

I. INTRODUCTION

There exists a large number of reports on the studies of the electronic structure of both elemental (Si and Ge) and compound semiconductors (mainly III-V) by means of angle-resolved photoelectron spectroscopy. By comparison with theoretical results it has been possible to achieve, to some extent, an understanding of the bulk and surface electronic structure. It is noteworthy, however, that despite these efforts there is still not one single semiconductor surface for which a one-to-one correspondence between experimentally and theoretically derived surface states has been obtained.[1] On the experimental side the major obstacle in this context is the problem of identifying the surface-derived spectral features. In particular, photoemission from band edges may in many cases be difficult to distinguish from surface-state emission. In a recent study[2] of CdTe(110) we found several features, some of which were previously unreported, which we assigned to surface states and resonances. Since the electron structures of different zinc-blende crystal compounds are generally very similar, one may hope that systematic comparison of data from different systems should resolve some of the ambiguities. In the spirit of this strategy, we present here a parallel study of the ZnTe(110) surface.

Reports on electron structure studies of ZnTe are scarce.[3,6] In a photoemission and electron-energy-loss investigation of clean and oxidized (110) surfaces,[5,6] concentrated on the location of the empty and occupied dangling-bond states, it was shown that these states are located outside the band gap as expected for relaxed surfaces. Among the theoretical efforts, Beres *et al.*[7] have calculated the surface electronic structure throughout the surface Brillouin zone (SBZ), emphasizing the importance of surface resonances versus bound surface states. Due to the lack of experimetnal data no comparison between theory and experiment could be made.

II. EXPERIMENT

The experiments were carried out at the toroidal grating mirror beamline of the MAX storage ring.[8] The ZnTe crystals, $4\times4\times10$ mm^3 in size, were obtained from Cleveland Crystals Inc, and characterized as "low resistivity." They were cleaved in an UHV preparation chamber ($p\approx5\times10^{-10}$ Torr) using a commercial cleaver (Kratos WG-186), with the knife edge perpendicular to a [111] direction to produce a (110) surface. The sample so obtained was transferred to a surface analytic system ($p\approx1\times10^{-10}$ Torr), containing a goniometer mounted hemispherical electron-energy analyzer, and a low-energy electron-diffraction system (LEED). The latter was used for checking surface quality and for azimuthal surface orientation. The LEED pattern showed sharp spots on a low background intensity.

The light, mainly p polarized, was kept at a constant angle of incidence of 45° relative to the surface normal. When not stated otherwise, the spectra were recorded in the plane of incidence of the light. All photoemission data were recorded after LEED characterization, which means that possible electron-beam-induced surface deterioration has not been investigated.[9] The initial band bending was not checked, but it was clear that the Fermi-level position remained unchanged throughout the experiments.

III. RESULTS

For mapping the bulk valence along the ΓKX direction, we have recorded normal-emission spectra in the photon energy range 17–100 eV. We have also measured off-normal-emission spectra using photon energies in the range of 23–41 eV for studies of surface related features. These data were taken along the boundaries of the SBZ, i.e., in the $\bar{\Gamma}\bar{X}$, $\bar{\Gamma}\bar{Y}$, $\bar{X}\bar{M}$, and $\bar{Y}\bar{M}$ directions. A selection of the results is shown in Figs. 1–6. For reference, we show in Fig. 7 the relation between the (110) surface and bulk Brillouin zones for a zinc-blende lattice.

IV. ANALYSIS AND DISCUSSION

A. Normal emission and mapping of bulk bands

Many features in the normal-emission spectra can be associated with direct interband transitions from initial

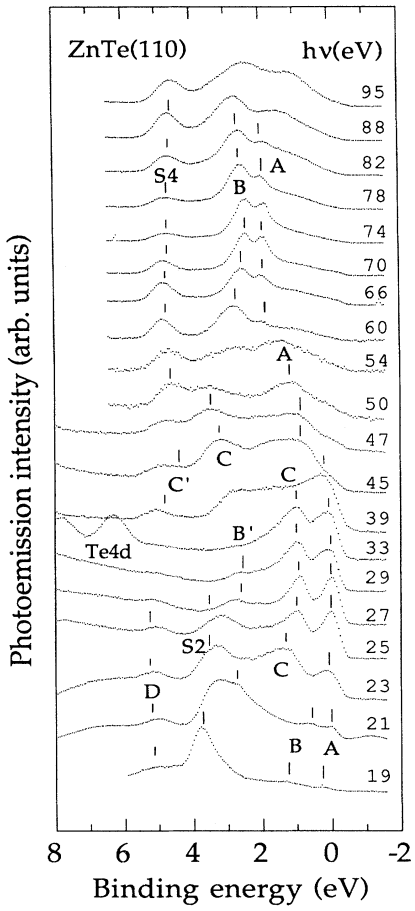

FIG. 1. Normal-emission photoelectron spectra from ZnTe(110) in the 19–95-eV range. The spectra are normalized to equal maximum amplitudes. The letters $A-D$ refer to identification in terms of interband transitions.

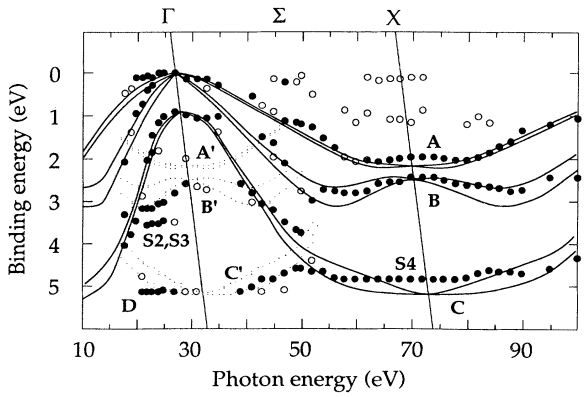

FIG. 2. Structure plot showing the peak positions in Fig. 1 (the same notations are used). The solid lines correspond to a bulk band-structure calculations performed in this work. The dotted lines are obtained assuming "umklapp processes"; see the text.

bands along the Σ line, i.e., the ΓKX direction. Using a sufficiently large range of photon energies we can determine energies at the Γ, K, and X points. This is done by observing extrema in binding energies with varying photon energy and by fitting the observed dispersion curvatures with calculated ones. The critical energies obtained were used for adjustment of the electron energy bands calculated with a semiempirical linear combination of atomic orbitals (LCAO) method,[10] including spin-orbit interaction. Once these bands are established, they are employed for analysis of the off-normal-emission spectra.

Measured normal-emission angle-resolved energy distribution curves (AREDC's) in the photon energy range 19–95 eV are shown in Fig. 1. In the energy range ~30–40 eV the valence-band emission partially overlaps with Te(4d) emission, excited in second order [e.g., the two peaks ~6–8 eV below the valence-band maximum (VBM) in the 33-eV spectrum]. The relevant spectral peak positions have been condensed to a band-structure plot, Fig. 2, where the solid and open circles represent well-defined peaks and weaker structures, respectively.

For the analysis we assumed direct transitions between our calculated LCAO initial states and free-electron-like states described by $E(\mathbf{k})=\hbar^2|\mathbf{k}-\mathbf{g}|^2/2m$. An inner potential of 5 eV relative to the VBM was deduced from the fact that the VBM (observed as the maximum emission energy in the spectra) is found at 27-eV photon energy, and from a general fitting of calculated band-structure plots (see below) to the experimental ones. Reciprocal-lattice vectors $\mathbf{g}=2\pi n(2,2,0)/a$, with $n=-1,1,2$, were used, i.e., so-called "primary transitions" were assumed to dominate. The corresponding calculated band-structure plot is shown as solid lines in Fig. 2. Transitions with g vectors not parallel to the surface normal ("umklapp transitions") are expected to contribute with a lower intensity.[11] In cases where calculated bands are available high up in the conduction band, one finds that fitting of each umklapp band requires an adjusted inner potential, different from that of the primary band. The shifts amount typically to several electron volts. Furthermore, one finds that a satisfactory fitting can only be obtained within a limited energy range. The most prominent structure of this kind found in the spectra is the peak at ~3 eV below the VBM excited around 25-eV photon energy. This excitation occurs, according to our analysis, along the Σ line projected on $\bar{\Gamma}$ in the second SBZ, and the transition is observed in normal emission due to an umklapp process with $\mathbf{g}=[002]$ or [111]. The dotted lines in Fig. 2 are calculated [111]-type umklapp bands. They are included here just to show that it is reasonable to assume that umklapp transition can occur in this region. Around 22-eV photon energy the peak reflects excitations from the high-density-of-states region at $\Sigma_{\min}$, which explains the apparently stationary peak position. Other experimental structures away from the theoretical lines, which also can be ascribed to umklapp processes, are the features observed 0–1 eV below the VBM in the photon energy range 40–80 eV. Since the structures are quite weak, their precise energy positions are rather uncertain. However, we have clear indications that the energies are not constant with a changing

momentum component perpendicular to the surface, and consequently they cannot be directly associated with surface states. We will not discuss these features any further in this paper.

We conclude that it is possible to obtain fair agreement between theory and experiment with respect to the bulk bands. This allows us to determine, by extrapolation, some critical point energies from the LCAO bands; see Table I. The results are compared with two recent band calculations.[12,13] Ekpenuma and Myles[12] performed a semiempirical tight-binding calculation which was fitted to experimental and theoretical data. References to older, less successful band calculations can be found in this paper. Bernard and Zunger[13] did a first-principles calculation and arrived at similar results. These two-band calculations agree with our results within 0.1–0.2 eV. At detailed comparisons of this kind one should keep in mind that *ab initio* band calculations usually refer to the ground state, while photoemission measures the excited state. The experimental binding energies are expected to be a few tenths of an eV larger than the theoretical ones.[14] In the case of (semi)empirical calculations these effects are of course absorbed in the parameters.

Around 70-eV photon energy the direct excitations occur near the zone boundary at X. Due to the high joint density of states, structures corresponding to direct transitions are strongly enhanced. Therefore it would appear that the peak ~ 4.8 eV below the VBM could be associated with emission from the X_6 point, though this would imply a significantly smaller bandwidth than the ~ 5.2 eV found in band calculations.[13] Generally, experimental peak positions corresponding to excitations from band extrema are expected to deviate somewhat from the true extreme energies as an effect of momentum and energy broadening due to limited lifetime and coherence length in the excited state, in combination with finite experimental angular resolution. Since the X_6 point defines the bottom of a dispersing energy band, one might suspect that a reduced measured binding energy is caused by such effects. A quantitative estimate, carried out in a similar way as discussed by Jezequel *et al.*,[15] shows, however, that due to the flat character of the bands around the X point, the deviation of the observed peak position from the true band extremum is estimated only as ~ 0.1 eV. We have also examined the possible effects of surface misorientation (i.e., assumed that the data represent off-normal emission), but again, the flatness of the bands near X would imply a misorientation much larger than

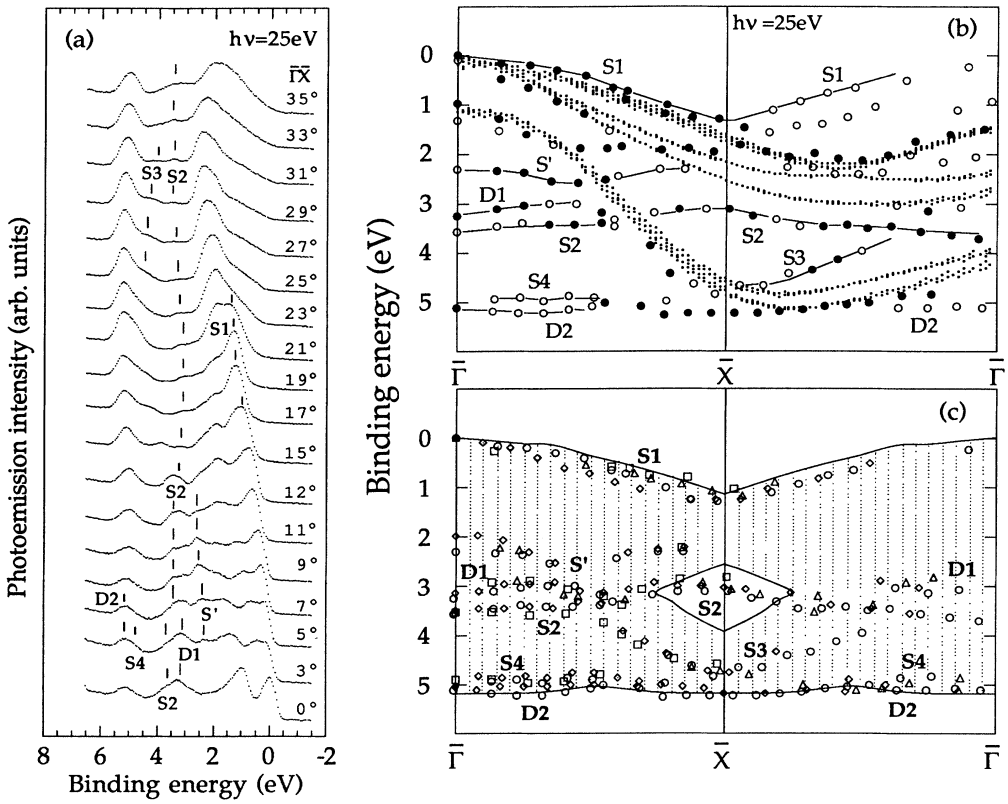

FIG. 3. (a) Normalized angle-resolved spectra in the $\bar{\Gamma}\,\bar{X}$ azimuth. $S1$–$S4$ denote surface-induced states, while $D1$ and $D2$ refer to density-of-states peaks. (b) The experimental peak positions in (a). The solid symbols represent well-defined peaks, while the open ones correspond to weaker features (e.g., shoulders). Some data points are tentatively connected with solid lines. The dotted curves are calculated interband transitions. (c) Observed structures not associated with bulk interband transitions, together with the calculated projected density of states. Photon energies: ◇, 23 eV; ○, 25 eV; △, 31 eV; and □, 41 eV.

that defined by our experimental conditions ($\lesssim 2°$). We therefore conclude that the peak found near 4.8 eV below the VBM at high photon energies is of a different origin. Taking into account the already-mentioned effects of self-energy corrections,[14] identification of the 4.8 eV peak with the X_6 point would imply an even larger discrepancy relative to the calculated bandwidth.

From spectra obtained with lower photon energies (25–40) eV, we do in fact find that the peak around 5 eV contains two contributions, one from the band minimum at ~ 5.2 eV and one at ~ 4.8 eV. From the off-normal data discussed below, it is clear that the maximum binding energy for the dispersing bands is rather close to 5.2 eV relative to the VBM. There are two other obvious possibilities to explain the structure at 4.8 eV. One is that it reflects another high density of states in this energy region, namely that at the L point (L_6). However, in normal emission from a (110) surface, for a contribution from the L point to be observed, one must invoke relaxation of the momentum conservation rule in all three dimensions, not only perpendicular to the surface. Such "density-of-states" features are generally not found with significant amplitudes in uv excited photoemission. The second possibility is that the structure represents surface-state emission. According to band-structure calculations,[7] the lowest cation derived surface state is expected to be located in this energy, slightly above the edge of the heteropolar gap. Qualitatively, the relatively enhanced surface-state emission at the higher photon energies could arise because of a reduced electron mean free path[16] (~ 10 Å at 15-eV and ~ 5 Å at 50-eV kinetic energy), though this particular state is localized on the second layer.[17] Thus is remains to be explained why the intensity of the X_6 emission at 5.2 eV appears relatively low (the large peak at 2.5 eV in the 70-eV spectrum derives from a state with the same X_6 symmetry). Finally, it should be noted that the deduced critical energies in Table I closer to the VBM are not affected by the identification of the X_6 point.

B. The $\bar{\Gamma}\,\bar{X}$ boundary

AREDC's in the $\bar{\Gamma}\,\bar{X}$ azimuth, obtained with 25-eV photon energy, are shown in Fig. 3(a) for a series of emission angles. From the set of data we have extracted a band-structure plot showing the binding energies as a function of the **k** vector parallel to the surface, $\mathbf{k}_{\parallel}$. The result is displayed in Fig. 3(b), where the same notations used in Fig. 2 are used here. As a guide for the identification, a theoretical band-structure plot was generated based on direct transitions between empirical LCAO initial bands and primary free-electron final bands, as described above [dotted lines in Fig. 3(b)].

Structures arising from direct bulk transitions can now

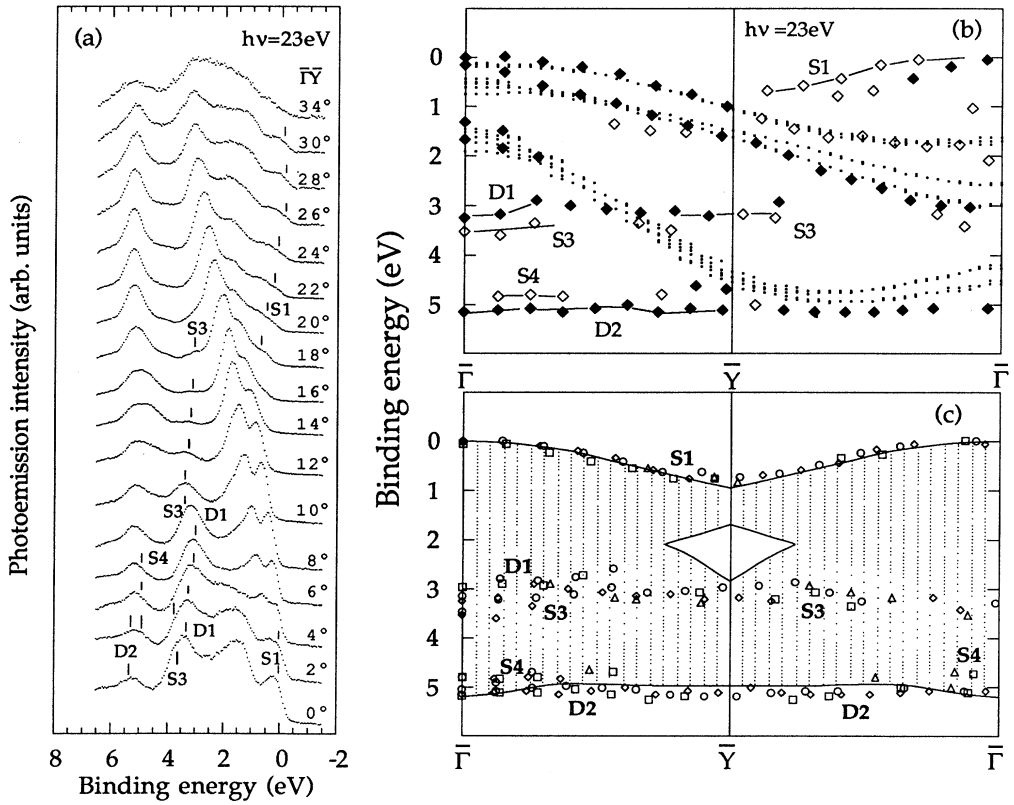

FIG. 4. Same as in Fig. 3, but along the $\bar{\Gamma}\,\bar{Y}$ zone boundary. Photon energies: ◇, 23 eV; ○, 25 eV; □, 27 eV; and △ 31 eV.

be interpreted by the comparison of the experimental and calculated dispersion curves, just as was done for normal emission. However, as the emission angle is varied, surface-induced states may disperse in a manner similar to that of nearby bulk states. The leading spectral peak in Fig. 3(a) ($S1$) represents such an ambiguous situation. Although its dispersion shows good agreement with the expected dispersion of the topmost bulk bands, the intensity of this peak reveals that the structure is actually surface related. As the boundary of the surface Brillouin zone is approached, the intensity undergoes an enhancement, but just as the $\bar{X}$ point is passed (near 20°), the intensity is rapidly reduced. Since the expected bulk interband transition occurs well off any zone boundary in this case (the zone boundary is reached at larger angles as indicated by the turning point in the calculated dispersion[10]), we do not expect any dramatic intensity variations in bulk derived structures here. Transitions involving surface states, on the other hand, may well show abrupt intensity changes on passing a surface Brillouin-zone boundary due to change of the reciprocal-lattice vector involved in the excitation. According to the only available surface electron band calculation for the ZnTe(110) surface,[7] the uppermost surface state appears rather dispersionless—the energy difference between $\bar{\Gamma}$ and $\bar{X}$ is ~0.3 eV, as compared with ~1.2 eV in our data. In a parallel photoemission study of the CdTe(110) surface[18] we have found similarly large dispersion for the corresponding state. In the case of CdTe there is a recent surface-state calculation by Schmeits on CdTe(110),[19] which shows that the dispersion of the uppermost occupied surface state is indeed quite large (~1.2 eV) along the $\bar{\Gamma}\,\bar{X}$ zone boundary. The present results clearly indicate the need for a refined theoretical treatment of the ZnTe(110) surface.

The relatively strong peak at 3.2 eV in normal emission has already been associated with excitation at Σ_{min}. Off normal this peak shows a weak upward dispersion, just as the border between low and high projected density of states indicated in Fig. 3(c). We consequently label this feature $D1$ (density of states). On the high-binding-energy side of this peak we find a shoulder ($S2$), which develops into a clearer structure when the intensity of the $D1$ peak is reduced off normal. The dispersion of this structure is superimposed in Fig. 3(c) on the calculated projected bulk density of states for four different photon energies. We see that the energy of $S2$ is independent of photon energy. Around the $\bar{X}$ point it is definitely located within a gap in the calculated projected density of states. In Figs. 3(b) and 3(c) we also see that the disper-

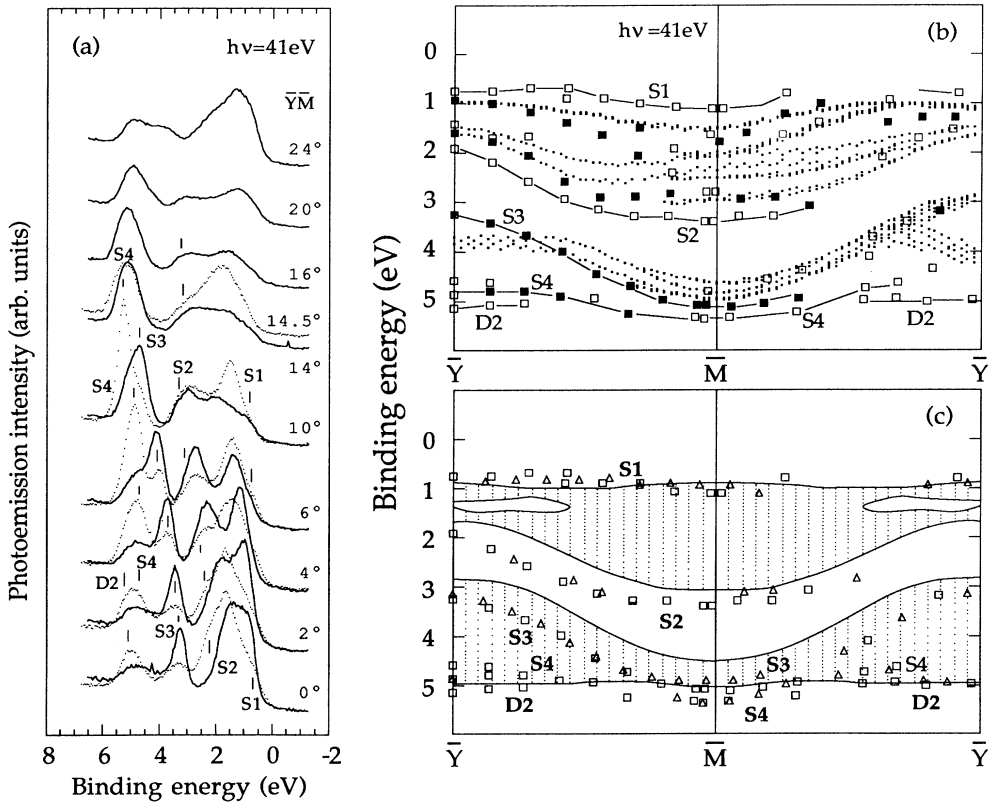

FIG. 5. (a) Photoemission spectra along the $\bar{Y}\,\bar{M}$ zone boundary, recorded for two polarization geometries: $\bar{E}$ parallel to $\bar{Y}\,\bar{M}$ (solid lines) and $\bar{E}$ perpendicular to $\bar{Y}\,\bar{M}$ (dotted lines). Emission at 0° represents $\bar{Y}$, while the $\bar{M}$ point is probed around 14°. All spectra represented with the true relative intensities. (b) and (c) as in Fig. 3. Photon energies: △, 31 eV; □, 41 eV.

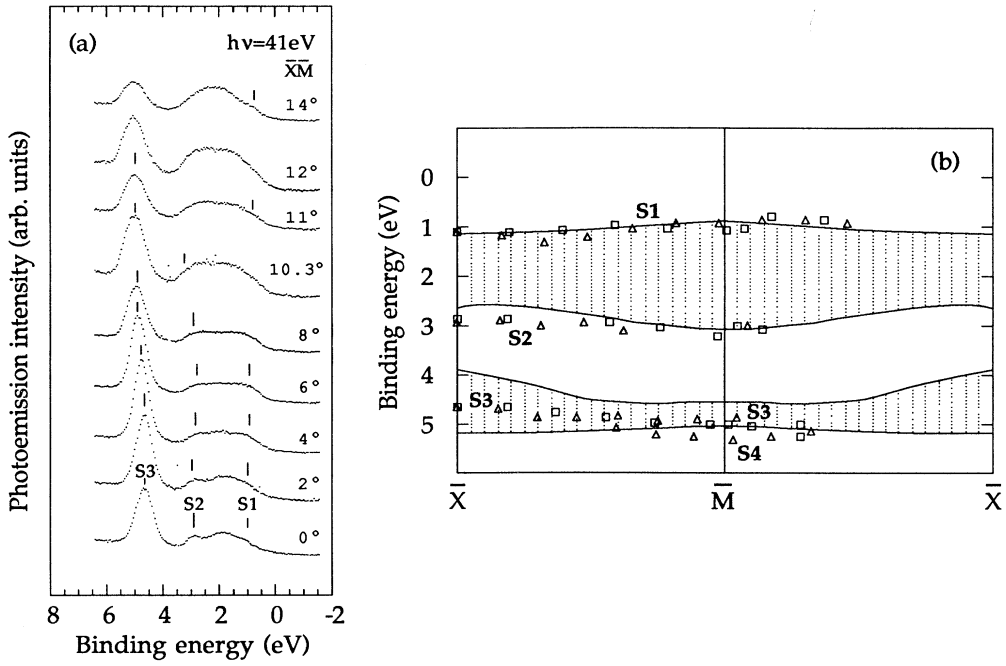

FIG. 6. (a) Photoemission spectra along the $\bar{X}\,\bar{M}$ zone boundary, obtained with $\bar{E}$ parallel to $\bar{X}\,\bar{M}$. 0° corresponds to emission from $\bar{X}$ (cf. Fig. 3), 10° to emission from $\bar{M}$. (b) Positions of surface-induced structures together with the calculated projected density of states. Photon energies: △, 31 eV; □, 41 eV.

sion of $S2$ is symmetric around the $\bar{X}$ point, which means it has the periodicity of the SBZ. All these observations show that $S2$ has the characteristics of a surface-state resonance.

Another weak structure $S3$, not accounted for by the calculated bulk interband transitions, is observed clearly at large emission angles. As the photon energy is changed, the relative intensity of this structure is rapidly reduced. In our recent study of CdTe(110),[2] we could, however, track a corresponding structure with different photon energies and could thus assign it to a surface resonance. From the general similarity between the electron structures of the two materials we assign $S3$ to a surface resonance. Within the experimental resolution $S2$ and $S3$ appear to be degenerate at $\bar{\Gamma}$.

A small peak S' is found at about 2.2-eV binding energy at normal emission and can be traced up to almost the zone boundary, i.e., the $\bar{X}$ point. Its dispersion is independent on the photon energy within the experimental uncertainty and we tentatively assign it to a surface resonance. It is, however, not predicted by theory.[7]

At small emission angles ($\lesssim 11°$) the peak at ~ 5 eV is quite broad, indicating the presence of two components. The lowest component $D2$ at ~ 5.2 eV binding energy is interpreted as a band-edge emission. We note that the peak tracks well the edge of the calculated projected density of states [see Fig. 3(c)]. This lends support to the above assignment to the X_6 point. The upper component at ~ 4.8 eV is interpreted as a surface resonance as discussed in connection with normal-emission data.

C. The $\bar{\Gamma}$ $\bar{Y}$ boundary

Figure 4(a) shows AREDC's measured at 23-eV photon energy in the $\bar{\Gamma}$ $\bar{Y}$ azimuth. The extracted peak positions are presented in a band-structure plot, Fig. 4(b), together with the corresponding theoretical plot for direct bulk excitations. Again some peaks can be directly attributed to bulk interband transitions, some cannot. Just as in the

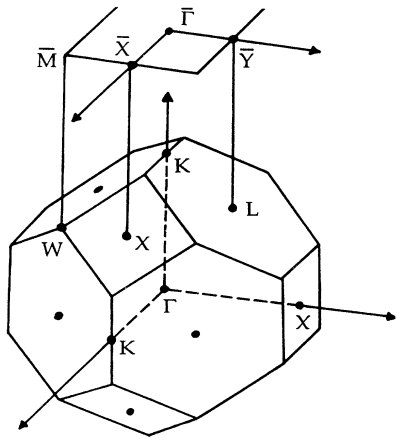

FIG. 7. Relation between bulk and surface Brillouin zones for a (110) surface of the fcc lattice.

TABLE 1. Comparison between critical point energies of our semiempirical LCAO band structure (fitted to agree with photoelectron energy distributions measured at normal emission in the photon energy range of 17–100 eV) and results from other band calculations.

	Γ_7	X_7	X_5	X_6	X_7	$L_{4,5}$	L_3	L_6	L_6
Theory[a]	0.9	2.1		2.3	5.3	1.0		1.4	5.0
Theory[b]			2.3		5.1		0.9		5.3
This work	0.9	2.2		2.5	5.2	0.9		1.5	5.0

[a]Reference 12.
[b]Reference 13.

$\bar{\Gamma}\,\bar{X}$ azimuth we find that the intensity of the uppermost peak is significantly reduced on passing the surface zone boundary at $\bar{Y}$, suggesting that the peak contains a surface derived component. Away from normal emission the $\Sigma_{\min}$ peak is tracking the upward dispersing projected-density-of-states border [$D1$ in Figs. 4(b) and 4(c)]. A structure $S3$, appearing as a shoulder on the high-binding-energy side of $D1$ at normal emission, does not correspond to any bulk transition. In Fig. 4(c) we see that the spectral position of $S3$ is independent of photon energy, so the structure is likely to be of surface origin. We tentatively regard it as the continuation of the resonance $S3$ found in the $\bar{\Gamma}\,\bar{X}$ azimuth. We use the same labeling for structures that we associate with the same initial state in different phase-space regions. In Fig. 4(c) we also see that the uppermost peak at $\bar{Y}$ appears above the edge of the projected density of states. It probably corresponds to one of the predicted anion derived surface states.[7] The lowest peak $\sim$5 eV has the same appearance as in the $\bar{\Gamma}\,\bar{X}$ azimuth, i.e., it contains the two components $D2$ and $S4$.

D. The $\bar{Y}\,\bar{M}$ boundary

Measurements along the two remaining zone boundaries were performed maintaining the p-polarization geometry and turning the analyzer outside the incidence plane. Spectra recorded around the $\bar{Y}$ point revealed that the relative intensity of the $S3$ peak is enhanced at higher photon energies (40–50 eV), particularly with the light polarized along the $\bar{Y}\,\bar{M}$ direction. A set of spectra obtained with 41-eV photon energy is shown in Fig. 5(a). The effect of changed light polarization is demonstrated for a couple of cases. The 0° settings correspond to emission from the $\bar{Y}$ point, while emission from the $\bar{M}$ point is reached at about 14.5°. Figures 5(b) and 5(c) show the calculated bulk interband transitions and the projected density of states along $\bar{Y}\,\bar{M}$. Focusing the attention to surface-related structures, we find four features $S1$–$S4$ which we do not identify with bulk interband transitions. The $S1$ and $S2$ features are overlapping bulk derived peaks and appear as relatively weak structures, though their existence is clear. In particular we see that the $S1$ peak emerges as a clear shoulder ($\sim$0.8 eV below the VBM) when excited with light polarized orthogonal to the $\bar{Y}\,\bar{M}$ direction. $S1$ seems to be above the projected density of states at $\bar{Y}$ but below at $\bar{M}$. There is, however, an uncertainty in both experiment and theory which makes this statement only tentative. The results support anyway the theoretical prediction of nearly nondispersive surface states just above the VBM and a downwards dispersing state near the upper part of the open "lens" in the projected density of states.[7]

The most pronounced surface-related structure is $S3$, dispersing just below the lower edge of the open lens (i.e., within the projected-density-of-states region). Just as in the $\bar{\Gamma}\,\bar{Y}$ azimuth, it can be observed at the same energy with a series of different photon energies, as expected for a surface resonance. We find also that the intensity of $S3$ is considerably larger when excited with the light polarized parallel to the $\bar{\Gamma}\,\bar{X}$ direction. Another resonance type of state is observed near the heteropolar gap ($S4$). Contrary to $S3$, the intensity of $S4$ is strongest when excited with the light polarized orthogonal to the $\bar{\Gamma}\,\bar{Y}$ direction. We note that in the vicinity of $\bar{M}$ the $S4$ state falls within the heteropolar gap, confirming its surface origin. Since $\bar{Y}$ is located on a mirror plane, one can conclude that at $\bar{Y}$ the symmetry of $S1$ and $S3$ with respect to this plane is odd, while that of $S4$ is even.

E. The $\bar{X}\,\bar{M}$ boundary

Figure 6(a) shows the final series of spectra, namely along the $\bar{X}\,\bar{M}$ boundary, obtained with 41-eV light polarized along $\bar{X}\,\bar{M}$. The angular scale is such that 0° corresponds to emission from $\bar{X}$, and the $\bar{M}$ point is reached near 10°. With the identifications of surface-induced structures along the other three zone boundaries, it is now fairly easy to identify the surface-related electronic structures along this one. $S3$ shows up again as the strongest spectral peak, and $S2$ appears in the gap region [see Fig. 6(b)]. The energy positions at the $\bar{M}$ and $\bar{X}$ points for $S2$ and $S3$ match well with the positions we observed both in the $\bar{\Gamma}\,\bar{X}$ as well as the $\bar{Y}\,\bar{M}$ direction. Approaching the $\bar{M}$ point a structure ($S4$) emerges within the heteropolar gap, just as along the $\bar{Y}\,\bar{M}$.

V. SUMMARY

The data presented above illustrate well some of the difficulties in detecting and identifying surface-induced structures in valence-band spectra from semiconductors. In many cases they show up as weak features, which disperse in a similar way as nearby direct bulk interband transitions or edges in the projected density of states. For instance, in the $\bar{\Gamma}\,\bar{Y}$ direction we could expect to ob-

serve the $S2$ surface resonance, but in that region we also expect emission from the high bulk density-of-states edge probably with the same dispersion. In the same way the $S1$ emission along the $\bar{\Gamma}\bar{X}$ and $\bar{\Gamma}\bar{Y}$ directions is mainly revealed by the intensity changes at the $\bar{X}$ and $\bar{Y}$ points. Nevertheless, through measurements along the four boundaries of the surface Brillouin zone we are able to extract a consistent (though not complete) overall picture of the surface electron energy bands; see Fig. 8.

Comparing the experimentally derived surface bands with those predicted theoretically by Beres *et al.*,[7] we find sufficient similarities to make tentative identifications. The comparison is, however, complicated by the fact that the bulk bands differ, as manifested by the projected density of states. Near the VBM there are theoretically two states which are p-like and localized on the Te atoms. The lower one A_4 is a back-bond state while the upper one A_5 is a dangling-bond state. Near the zone center they are resonant (below the VBM), while around the $\bar{M}$ point they are in the band gap. Experimentally only one state ($S1$) is observed. It follows very closely the projected band edge. In the region around the $\bar{X}$ point we find a significantly larger dispersion for $S1$ than predicted by the calculation of Beres *et al.*[7] A similarly large dispersion is observed for CdTe.[18] We note that in a recent calculation on CdTe(110) by Schmeits,[19] the dispersion of the anion-derived dangling-bond state is found to be of similar magnitude in the region of $\bar{X}$ to that observed here for ZnTe. The $S2$ state is identified with theory state A_3. This state is p-like and localized on the second-layer Te atoms. Both $S2$ and A_3 disperse in a similar way along the upper part of the forbidden "lens" region. However, along $\bar{\Gamma}\bar{X}$ we have experimentally an upward dispersion while a downward dispersion is found theoretically. The $S3$ structure corresponds to the C_2 state, which is s-like and localized on the zinc atom. The dispersions agree qualitatively. C_2 is a pure surface state (in the lens gap), while $S3$ is a resonance. This may be connected with the fact that the lens gap is much broader in theory than experimentally. The $S4$ structure should be associated with the C_1 state. This is similar to C_2 but located in the second layer. At the $\bar{M}$ point we find it below the valence band while it is a resonance in theory. Finally we observe a state S' in the $\bar{\Gamma}\bar{X}$ direction, which is not immediately identifiable. Possibly it could be an extension of A_2' or A_1' found at the $\bar{X}$ point in theory.

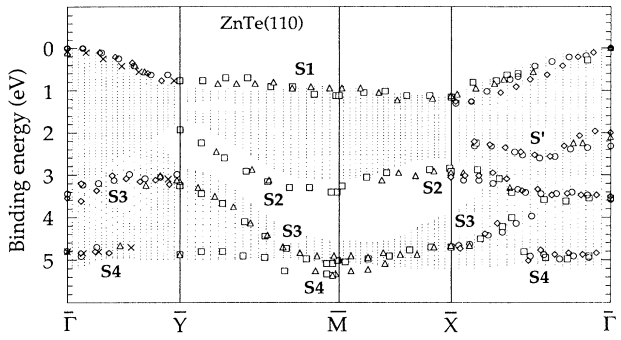

FIG. 8. Dispersion trajectories of the surface-related structures obtained in this work together with the calculated projected bulk density of states. Photon energies: ◇, 23 eV; ○, 25 eV; × 27, eV; △, 31 eV; and □, 41 eV.

Because of uncertainties in both theory and experiment the discussed assignments must be regarded as tentative. Complementary experiments where the surface states are tested by adsorbates are planned. Calculations of the surface electronic structure are in progress.

ACKNOWLEDGMENTS

We wish to thank the staff at MAX-lab for the generous technical assistance. Financial support from the Swedish Natural Science Research Council is gratefully acknowledged.

[1]G. V. Hansson and R. I. Uhrberg, Surf. Sci. Rep. **9**, 197 (1988).
[2]H. Qu, J. Kanski, P. O. Nilsson, and U. O. Karlsson, J. Electron Spectrosc. Relat. Phenom. **52**, 149 (1990); H. Qu, J. Kanski, P. O. Nilsson, and U. O. Karlsson, Vacuum **41**, 610 (1990).
[3]J. L. Shay and W. E. Spicer, Phys. Rev. **175**, 741 (1968).
[4]N. J. Shevchik, J. Tejeda, M. Cardona, and D. W. Langer, Phys. Status Solidi B **59**, 87 (1973).
[5]Y. Suda, A. Ebina, and T. Takahashi, Rec. Electron. Commun. Eng. Conversazione Tohoku Univ. **49**, 18 (1980).
[6]T. Takahashi and A. Ebina, Appl. Surf. Sci. **11/12**, 268 (1982).
[7]R. P. Beres, R. E. Allen, and J. D. Dow, Phys. Rev. B **26**, 769 (1982).
[8]U. O. Karlsson, J. N. Andersen, K. Hansen, and R. Nyholm, Nucl. Instrum. Methods A **282**, 553 (1989).
[9]T. P. Humphrey, G. P. Srivastava, and R. H. Williams, J. Phys. C **19**, 1259 (1986).
[10]H. Qu, P. O. Nilsson, J. Kanski, and L. Ilver, Phys. Rev. B **39**, 5276 (1989).
[11]G. D. Mahan, Phys. Rev. B **2**, 4334 (1970), and J. Henk, W. Schattke, H. -P. Barncheidt, C. Janowitz, R. Manzke, and M. Skibowski, *ibid.* **39**, 13 286 (1989).
[12]S. N. Ekpenuma and C. W. Myles, J. Phys. Chem. Solids **51**, 93 (1990).
[13]J. E. Bernard and A. Zunger, Phys. Rev. B **36**, 3199 (1987).
[14]See, e.g., R. W. Godby, M. Schlüter, and L. J. Sham, Phys. Rev. B **37**, 10 159 (1988).
[15]G. Jezequel, A. Barski, P. Steiner, F. Solal, P. Roubin, R. Pinchaux, and Y. Petroff, Phys. Rev. B **30**, 4833 (1984).
[16]D. P. Woodruff, *The Chemical Physics of Solid Surfaces and Heterogeneous Catalysis,* edited by D. A. King and D. P. Woodruff (Elsevier, Amsterdam, 1981), Vol. 1, p. 81.
[17]J. R. Chelikowsky and M. L. Cohen, Phys. Rev. B **20**, 4150 (1979).
[18]Qu Hua, J. Kanski, P. O. Nilsson, and U. O. Karlsson (unpublished).
[19]M. Schmeits, Surf. Sci. **231**, 389 (1990).